Contents lists available at ScienceDirect

Toxicon: X

journal homepage: www.journals.elsevier.com/toxicon-x

Development of a membrane-disruption assay using phospholipid vesicles as a proxy for the detection of cellular membrane degradation

Mátyás A. Bittenbinder [a,b,c], Eric Wachtel [b], Daniel Da Costa Pereira [d], Julien Slagboom [b,c], Nicholas R. Casewell [e], Paul Jennings [d], Jeroen Kool [b,c,1,*], Freek J. Vonk [a,b,c,1]

[a] *Naturalis Biodiversity Center, Leiden, the Netherlands*
[b] *AIMMS Division of BioAnalytical Chemistry, Department of Chemistry and Pharmaceutical Sciences, Faculty of Sciences, Vrije Universiteit Amsterdam, Amsterdam, the Netherlands*
[c] *Centre for Analytical Sciences Amsterdam (CASA), Amsterdam, the Netherlands*
[d] *AIMMS Division of Molecular and Computational Toxicology, Department of Chemistry and Pharmaceutical Sciences, Vrije Universiteit Amsterdam, Amsterdam, the Netherlands*
[e] *Centre for Snakebite Research & Interventions, Liverpool School of Tropical Medicine, Liverpool, United Kingdom*

ARTICLE INFO

ABSTRACT

Snakebite envenoming is a global health issue that affects millions of people worldwide, and that causes morbidity rates surpassing 450,000 individuals annually. Patients suffering from snakebite morbidities may experience permanent disabilities such as pain, blindness and amputations. The (local) tissue damage that causes these life-long morbidities is the result of cell- and tissue-damaging toxins present in the venoms. These compounds belong to a variety of toxin classes and may affect cells in various ways, for example, by affecting the cell membrane. In this study, we have developed a high-throughput *in vitro* assay that can be used to study membrane disruption caused by snake venoms using phospholipid vesicles from egg yolk as a substrate. Resuspended chicken egg yolk was used to form these vesicles, which were fluorescently stained to allow monitoring of the degradation of egg yolk vesicles on a plate reader. The assay proved to be suitable for studying phospholipid vesicle degradation of crude venoms and was also tested for its applicability for neutralisation studies of varespladib, which is a PLA$_2$ inhibitor. We additionally made an effort to identify the responsible toxins using liquid chromatography, followed by post-column bioassaying and protein identification using high-throughput venomics. We successfully identified various toxins in the venoms of *C. rhodostoma* and *N. mossambica,* which are likely to be involved in the observed vesicle-degrading effect. This indicates that the assay can be used for screening the membrane degrading activity of both crude and fractionated venoms as well as for neutralisation studies.

1. Introduction

An estimated 1.8–2.7 million snakebites occur annually, resulting in over 100,000 fatalities and more than 450,000 victims suffering from permanent physical damage (Gutié et al., 2017). Snake venoms are complex mixtures containing numerous toxins from various protein families, which possess a variety of activities and clinical effects. The three main pathologies in snakebite victims include haemotoxicity, neurotoxicity and tissue-damaging activities (Gutiérrez et al., 2017; Kasturiratne et al., 2008; Habib et al., 2015; Warrell, 2010). Although

the latter is not the most life-threatening, the tissue-damaging effects are one of the leading causes of life-long morbidities (Gutiérrez et al., 2017; Warrell, 2010; Longbottom et al., 2018; Chippaux, 2017). Therefore, it is surprising that considerably less research has been performed on the tissue-damaging effects compared to the research that has been done on the haemotoxic and neurotoxic venom effects (Bénard-Valle et al., 2015; Gutiérrez et al., 2017). The cell- and tissue-damaging activities of snake venoms are caused by a variety of toxins. These include hydrolytic enzymes (e.g., phospholipases A$_2$ (PLA$_2$s), snake venom metalloproteinases (SVMPs) and hyaluronidases), as well as β-defensins,

C-type lectin-like proteins (CTLs), disintegrins and cytotoxic three-finger toxins (3FTxs) (Fry, 2015; Gutiérrez et al., 2017; Gopalakrishnakone et al., 2017). These toxins possess various mechanisms by which they affect cells and tissues. These include 'direct' cytotoxins, which affect the cells by disrupting or destabilising the plasma membrane, and toxins that affect the cells 'indirectly' by damaging the extracellular matrix (Bittenbinder et al., 2023; Gutiérrez et al., 2016, 2017; Markland and Swenson, 2013; Montecucco et al., 2008; Gasanov et al., 2014; Sunagar et al., 2013). The plasma membrane performs an essential role in normal cell functioning and forms an integral part of the cell (Alberts et al., 2018). This could explain the fact that various toxin families target the cell membrane to achieve their cell-damaging effects.

Several assays have been developed over the years that can be used to study the membrane-degrading activity of snake venoms. Cell culturing assays are used to study the effect of certain toxins on cell membrane integrity and cell viability. In addition to cell-based assays, a number of methods exist that have been used to study the activity of toxins targeting the cell membrane. Some of these assays rely on the release of free fatty acids as a result of hydrolysis of phospholipids, resulting in an acidification of the reaction mixture (Condrea et al., 1962; Still et al., 2020; Price, 2007). Others include turbidity assays that use egg yolk emulsions, in which a decrease in turbidity is used as a measure for membrane degrading activity (Marinetti, 1965; Joubert and Taljaard, 1980; Senji Laxme et al., 2019; Doley et al., 2004). With the latter, a decrease in turbidity is caused by the fact that certain venoms and their toxins degrade the egg yolk vesicles. The lipid vesicles structurally resemble the membrane of living cells and could, therefore, be used as a proxy for membrane degrading activity (Marinetti, 1965; Monteiro et al., 2014). Although practical, these turbidity assays were mainly used for studying crude venoms and require relatively large sample volumes (Marinetti, 1965; Joubert and Taljaard, 1980; Senji Laxme et al., 2019, 2021).

In this study, we describe the development of a low assay volume high-density well plate (i.e., 384-wells) based vesicle degradation (VD) assay that uses fluorescently dyed phospholipid vesicles to study membrane degradation of both crude snake venoms and fractionated venom toxins. The size of the vesicles created by resuspending the egg yolk was not formally characterised and probably contains multiple forms of phospholipid vesicles, including micelles and liposomes (Oladimeji and Gebhardt, 2023; Abeyrathne et al., 2022; Strixner et al., 2014; Dennis et al., 2011). By fluorescently staining these vesicles, we were able to quantify the membrane degrading activity in terms of a decrease in fluorescence signal, which was done in a high-throughput manner on a fluorescence plate reader. After optimisation and validation of the assay using crude venoms, the assay was integrated into nanofractionation analytics. With nanofractionation analytics, the venoms are subjected to chromatographic separation using reversed-phase chromatography (RP-HPLC) (Mladic et al., 2017; Slagboom et al., 2017; Zietek et al., 2018). This is followed by toxin fractionation on 384-well plates for subsequent bioassaying and toxin identification with high-throughput (HT) venomics (Slagboom et al., 2023; Palermo et al., 2023). Although some studies have investigated the membrane degrading effect of purified toxins on egg yolk vesicles, this study involves the fractionation of multiple venoms followed by post-column bioassaying of fractionated toxins for their membrane degrading activity (Doley et al., 2004; Fernandes et al., 2014).

The assay was optimised by evaluating various parameters, including egg yolk concentration, well volumes, egg yolk buffer preparation methods, microwell plate types and plate reader types. After optimisation, the assay was validated using the venoms of a panel of medically relevant venomous snake species. The results show that the assay could be used for studying vesicle degradation by crude venoms and was also tested for its applicability in neutralisation studies. After studies with crude venoms, we set out to identify the bioactive compounds that were capable of vesicle degradation. These data showed a substantial decrease in fluorescence signal (i.e., indicating degradation of the

vesicles) by specific venom components. Subsequent toxin characterisation by HT venomics revealed that the responsible venom components were likely to be phospholipase A_2s (PLA$_2$s). This suggests that the assay could be used to screen both crude and fractionated venoms, making it suitable for studying venom effects and for screening for possible inhibitory candidates for membrane degrading activities.

2. Material and methods

2.1. Chemicals and reagents

Ultrapure water was obtained through purification using a Milli-Q® Reference Water Purification System (Millipore). Dulbecco's phosphate buffered saline (no calcium, no magnesium, pH 7.0–7.3; PBS) was purchased from Thermo Fisher Scientific Inc. Tris-HCl buffer (50 mM, pH 7.4) was prepared with Trizma® base in ultrapure water and the pH was as adjusted using 1.0 M HCl. Egg yolk from chicken (powder), Trizma® base ($\geq$99.9 %), hydrochloric acid (ACS reagent, 37 %; HCl) and Triton™ X-100 (BioXtra) were obtained from Sigma-Aldrich. Hoechst 33342 (trihydrochloride, trihydrate - 10 mg/mL solution in water; Hoechst) nucleic acid stain was obtained from Invitrogen™ by Thermo Fisher Scientific Inc., Gibco™. For the neutralisation assays, varespladib (Sigma-Aldrich) was used as a PLA$_2$-inhibitor. Acetonitrile HPLC-R (ACN) and trifluoroacetic acid HPLC grade (TFA) were obtained from Biosolve B.V.

2.2. Venoms

Snake venoms were sourced from the venom library of the Faculty of Science, BioAnalytical Chemistry division, Vrije Universiteit Amsterdam (VU). This library contains samples from, amongst others, the Liverpool School of Tropical Medicine (LSTM), the National University of Singapore (NUS), and private keepers. The snake venoms used in this study came from the following viper (Viperidae) and elapid (Elapidae) species: *Bothrops jararaca* (jararaca, captive bred)*, Bungarus multicinctus* (many-banded krait, locality unknown)*, Calloselasma rhodostoma* (Malayan pitviper, Thailand), *Daboia russelii* (Russell's viper, locality unknown)*, Dendroaspis polylepis* (black mamba, captive bred), *Echis ocellatus* (West African carpet viper, Nigeria)*, Naja mossambica* (Mozambique spitting cobra, captive bred) and *Naja naja* (Indian cobra, captive bred). These species were selected as they represent some of the most medically relevant species across the geographical regions most heavily affected by snakebite (i.e., Latin America, Sub-Saharan Africa and Southeast Asia). Venoms were stored at −80 °C. Venom samples were reconstituted in ultrapure water to the desired concentrations. These solutions were then aliquoted and subsequently snap-frozen in liquid nitrogen and stored at −80 °C until use. All venoms used are in accordance with the Nagoya protocol, where applicable (Secretariat, 2011).

2.3. Method development

The assay is based on the principle that the fluorescent signal decreases in the presence of phospholipid vesicle-degrading proteins (e.g., snake venom toxins). This is caused by the fact that the fluorescence dye that was trapped in the vesicles is now released into the buffer solution, which results in lower fluorescence.

The formation of egg yolk vesicles is thought to occur due to the self-assembly of amphiphilic molecules in an aqueous solution. In these vesicles, the hydrophobic tails are shielded from the water while the hydrophilic heads interact with the aqueous environment (Monteiro et al., 2014; Nsairat et al., 2022). In an attempt to better visualise the vesicle degrading effect, we used Hoechst 33342 (Hoechst), which is known as a nucleic acid stain (Bucevičius et al., 2018; Lalande et al., 1981). Although Hoechst is generally used for cellular staining, we noticed that the vesicles were much better visible in the presence of this

stain (data not shown). Although the exact mechanisms are unknown, Hoechst (due to its lipophilic nature) probably gets entrapped in the lipid bilayer, thereby 'dyeing' the vesicles (Bucevičius et al., 2018; Lalande et al., 1981). This allowed us to measure the vesicle degrading activity in terms of a decrease in fluorescence signal, which could be done in a high-throughput manner on a fluorescence plate reader.

For the initial experiments, a clear 96-well F-bottom plate (Greiner Bio-One) was used. We first added 10 μL of sample to the wells (i.e., 10 μL of ultrapure water as a negative control, 10 μL of 20% Triton X-100 as a positive control or 10 μL venom), followed by adding 90 μL of egg yolk buffer. The egg yolk buffer was made by resuspending egg yolk from chicken (i.e., egg yolk powder) in PBS or Tris-HCl buffer to make a stock solution of 11 mg/mL egg yolk buffer (i.e. so that the final assay concentration would become ~10 mg/mL). Prior to resuspending the egg yolk in PBS or Tris-HCl, Hoechst was added to this buffer (diluted 1:20,000). The egg yolk buffer was homogenised by shortly shaking the emulsion prior to pipetting into a microwell plate. For these experiments, we used the venoms of four snake species (i.e., *B. jararaca*, *E. ocellatus*, *D. polylepis* and *N. mossambica*) at 100 μg/mL. The effects on the egg yolk vesicles were subsequently imaged using one of the fluorescence channels of the Operetta CLS high content imager (i.e., Ex: 355–385 nm, Em: 430–500).

2.4. Method optimisation

Egg yolk vesicle degradation was quantified using the decrease in fluorescence in response to venoms with membrane-disrupting activity. Degradation of the vesicle membrane would result in a decrease in relative fluorescence, which was monitored using a fluorescence plate reader (Varioskan™ LUX Multimode Microplate Reader 3020-444, controlled by SkanIt RE 4.1 software). The signal decrease was used as a proxy to monitor the membrane-degrading activity of the respective venom analysed. In order to make the assay useable for plate reader format, we evaluated various parameters, including egg yolk concentration, assay well volumes, egg yolk buffer preparation methods, microwell plate types and different plate reader types. The fluorescence signal was captured using an excitation wavelength of 355 nm and an emission wavelength of 460 nm. The degradation of egg yolk vesicles was monitored at 37 °C for 120 min (data captured every 2 min). Fluorescence was measured over time, and membrane-disrupting activity was expressed in relative fluorescence units (RFU). Triton X-100 was used as the positive control, and PBS was used as a negative control. For a detailed overview of the parameters that were assessed during optimisation, see Section 1 of the S1 Methods.

After optimisation, we continued further assaying with a total well volume of 50 μL by combining 5 μL of venom (at a concentration that is 10x pre-concentrated so that the final concentration would be 10x lower) with 45 μL of egg yolk buffer (final concentration ~10 mg/mL). For both controls, either 5 μL of 20% Triton X-100 (i.e., so that the final percentage of Triton X-100 was 2%) or 5 μL of PBS was used, followed by adding 45 μL egg yolk buffer. Measurements were done on 384 V-bottom plates (Greiner Bio-One) with the CLARIOstar PLUS Microplate reader (using bottom optic reading).

2.5. Validation of the VD assay using crude venoms

The assay was subsequently used to study the membrane-disrupting effects of a selection of eight snake venoms. For this, a serial dilution of each of the venoms was made (i.e., final concentrations of 100, 33.3, 11.1, 3.7, 1.2 and 0.4 μg/mL). These experiments were performed using the 384-well V-bottom plate. Each condition (positive control, negative control, and venom dilutions) was tested in triplicate. Plates were then measured at 37 °C, with data being captured every 10 min for a total of 12 h.

2.6. Testing the ability of the assay to be used for neutralisation studies

In order to test the applicability of the assay for neutralisation studies, we tested the neutralising capacities of varespladib, a PLA$_2$-inhibitor which is known for its capacity to neutralise both the enzymatic and catalytically inactive variants of PLA$_2$s (Bryan-Quirós et al., 2019; Salvador et al., 2019; Lewin et al., 2022). A serial dilution of the venoms was made (400, 133.3, 44.4, 14.8, 4.9, 1.6 μg/mL, 4x concentrated) which added to varespladib (4 μM, 4x concentrated) in a 1:1 ratio. This mixture was incubated for 30 min at 37 °C. We then pipetted 25 μL of the venom-varespladib mixture into a 384-V bottom plate and added 25 μL of egg yolk buffer (20 mg/mL, 2x concentrated). This resulted in final concentrations of 100, 33.3, 11.1, 3.7, 1.2 and 0.4 μg/mL for the venom, 1 μM for varespladib and 10 mg/mL for the egg yolk buffer. Next, the measurement on the CLARIOstar Plus Microplate reader was started at 37 °C. Data was captured every 10 min for a total of 12 h.

2.7. Identification of bioactive compounds in fractioned venoms

To elucidate which venom toxins are possibly associated with the degradation of the vesicle membranes, we used nanofractionation analytics to separate crude venoms into their individual toxins (Zietek et al., 2018; Mladic et al., 2016). We selected the venoms of the most potent species from each snake family, which were used for subsequent analysis (i.e., *C. rhodostoma* from the Viperidae family and *N. mossambica* from the Elapidae family). The nanofractionation approach includes chromatographic separation of the venom by reversed-phase chromatography (RP-HPLC), followed by the post-column VD assay in parallel with toxin identification using the HT venomics approach developed by Slagboom et al. (2023). Section 2.1 of the S1 Methods provides a more elaborate description of chromatographic separation and HT venomics.

After fractionation, the plates were evaporated overnight using a Christ Rotational Vacuum Concentrator RVC 2–33 CD plus (Salm en Kipp, The Netherlands). The plates were subsequently stored at −20 °C. Upon use, the fractions in each well were reconstituted in 50 μL of egg yolk buffer (10 mg/mL) by robotic pipetting using a ThermoFisher Multidrop. The plates were centrifuged at 1500 rpm at 20 °C for 60 s in a 5810 R centrifuge (Eppendorf AG). Each plate was then sealed (i.e., using Thermo Scientific Sealing Tape for 96-well plates) to avoid evaporation, and the plates were subsequently incubated at 37 °C. The well plates were then measured on the CLARIOstar Plus microplate reader at various time points (i.e., after 0, 2, 4, 8 and 16 h of incubation). Bioactivity chromatograms were generated by plotting the fluorescence readouts (in RFU) of the fractions on the y-axis against the retention time of fractionation on the x-axis. The baseline signal (i.e., showing no vesicle degrading effect) is represented on the y-axis at the beginning of each chromatogram, whereas the negative peaks (dips) correspond to bioactive fractions.

In an attempt to identify the toxins responsible for the negative peaks (i.e., representing membrane degrading activity), we performed the HT venomics method described by Slagboom et al. (2023) on both venoms that were fractionated on separate 384 V-bottom plates. Tryptic digestion was performed directly on the microwell plates, followed by MicroLC-MS/MS, which yielded proteomics data for each well. This data was converted into MGF files using ProteoWizard's msConvert (for details, see section 2.4 of the S1 Methods). Database searching was performed using the UniProt database containing only Serpentes (i.e., snake) accessions. Using multiple in-house written scripts, the database searches were first exported as comma-separated values (CSV) files (containing all information obtained from the database search). Using in-house written scripts, the relevant information from these files was then merged into a single Excel file containing the information of all toxins found in each well (e.g., protein accession numbers, protein scores, sequence coverages, and protein descriptions). Then, so-called protein score chromatograms (PSCs) were generated by plotting the protein score (y-axis) against the retention time (x-axis) for each toxin

found in the wells. Sections 2.2–2.4 of the S1 Methods provide a complete overview of the HT venomics workflow. For additional information on the scripts and data processing steps for HT venomics, see Slagboom et al. (2023). Lastly, the PSCs were then superimposed with the bioactivity chromatograms in order to correlate the bioactivity peaks with each snake venom fraction based on retention time and matching peak shapes. Graphs were drawn using GraphPad Prism version 9 (GraphPad Software, Inc.). We have previously described a similar workflow in more detail (Palermo et al., 2023).

2.8. Statistical analysis

All data was measured in triplicate and is represented by mean ± SD. For the neutralisation studies, the differences between venoms with and without inhibitors were assessed using a one-tailed test. Statistical analysis was performed using GraphPad Prism 9. Specific statistical tests used, p-value level definitions, and additional details are listed in the respective figure legends.

3. Results and discussion

3.1. Method development

In order to test the applicability of the vesicle degradation assay principle, we studied the vesicle degrading activity of the venoms of *B. jararaca*, *E. ocellatus*, *D. polylepis* and *N. mossambica*. Using a microscope with a fluorescence channel for Hoechst (i.e., Ex: 355–385 nm, Em: 430–500 nm) provided insights into how the vesicles were affected in the presence of venom. The addition of the venoms of *B. jararaca*, *E. ocellatus* and *N. mossambi*ca, for example, resulted in a clear decrease in the number o f vesicles (photographic images of these results are given in the supporting information figures S1 and S2). For *D. polylepis,* however, no visual reduction of vesicles was observed, even not after prolonged incubation (i.e., 2 h). This suggests that the venoms of *B. jararaca*, *E. ocellatus* and *N. mossambica* could have a membrane degrading activity, which results in the degradation of the vesicle membrane. A clear difference could further be observed when using PBS as a buffer compared to Tris-HCl buffer. With the latter, the contrast between wells in which the vesicles were affected was less apparent (S1 and S2 Figures).

3.2. Optimisation of the VD assay

As the vesicle degrading effects of certain venoms were clearly visible under the fluorescence microscope, we set out to see whether this decrease in fluorescence could also be measured on a fluorescence plate reader. For optimisation of the VD assay, a range of parameters was tested to make the assay reliable, robust and suitable for high-throughput screening of snake venoms on high-density, low-volume microwell plates. As the first parameters, we tested the concentration of the egg yolk emulsion and the appropriate well plate type. We compared seven concentrations of egg yolk emulsion (i.e., final concentrations of 20, 10, 5, 2.5, 1.25, 0.63 and 0 mg/mL) and three microwell plate types (i.e., clear 96-well flat-bottom, 384-well flat-bottom and 384-well V-bottom, for details see S1 Table). For the concentrations of the egg yolk emulsion, we observed that an egg yolk concentration of 10 mg/mL provides the highest RFU and the largest assay window (i.e., the difference in RFU between negative and positive control) (graphs of all concentrations and plate types tested are shown in S3 Figure).

In addition to the variation in RFU when using different egg yolk concentrations, apparent differences in RFUs for the assay windows between the controls could be observed between the three types of microwell plates. The data obtained from the 96-well F-bottom plate resulted in larger error bars compared to both 384-well plates tested (graphs provided in S3 Figure). The 384-well F-bottom plate produced a minor background noise, although the assay window between both

controls was smaller than with the other two microwell plates (graphs for the 384-well F bottom plate are shown in S3b Figure). In addition to showing smaller error bars compared to the other two plate types, the 384-well V-bottom plate gave the largest assay window between positive and negative control (S3c Figure). This well plate type was used for further assay optimisation.

To determine the optimal way of preparing the egg yolk buffer (i.e., to investigate whether various preparation methods would influence the assay window between negative and positive control), various ways of preparing the egg yolk buffer were tested. Slow shaking for 10–60 s once the egg yolk powder and PBS were combined gave the best results in terms of the homogeneity of the egg yolk emulsion and provided the smallest error bars and largest assay window between positive and negative control (S5 Figure). Fast shaking, vortexing (for >30 s), or sonication, on the other hand, seriously reduced the assay window between positive and negative control (S5 Figure). Slow shaking for ~10 s was found to provide the best results (i.e., this gave the largest assay window). The advantage of using this method for preparing the egg yolk emulsion is that it is straightforward and can be easily used when preparing larger stock solutions (e.g., more than 50 mL). We, therefore, continued the assay development using this preparation method.

The reaction volume was the next parameter that was optimised. In order to test this, end volumes of 10–100 μL were investigated, and measurements were done kinetically for 1 h at 37 °C. Reaction volumes of 30–50 μL gave the largest assay window when negative and positive controls were compared (graphs of the various reaction volumes provided in S4 Figure). For further optimisation, we selected 50 μL as the optimal assay volume, as this volume gave a proper assay window and because larger volumes will require more reagents.

As a final step in optimisation, in an effort to increase the assay window and minimise signal variation, we compared the differences in the results of two types of fluorescence plate readers. For this, we repeated the assay (positive vs. negative) on a 384-well V-bottom at 37 °C with all optimised parameters as mentioned above. We compared the readouts of the Varioskan™ microplate reader to that of the CLARIOstar *Plus* Microplate reader 430–4478 (BMG LABTECH), which is coupled to MARS data analysis software. For the CLARIOstar, we further compared top optic and bottom optic readings (as this option was only available to us in our CLARIOstar Plus), in addition to a number of other settings (i.e., focal height and gain). The largest window between positive and negative control was found when using the bottom reading on the CLARIOstar (for the differences between negative and positive control after 2 h of incubation, see S6 Figure). To summarise, for further experiments, we used the following parameters: 1) final concentration of 10 mg/mL egg yolk in a buffer on a 384 V-bottom microwell plate; 2) slow shaking for ~10 s as a preparation method; 3) assay volume of 50 μL; 4) bottom reading on the CLARIOstar microplate reader.

3.3. Validation of the VD assay using crude venoms

To validate the proposed assay method for screening the effects of snake venoms on the vesicles, we selected venoms from a panel of medically relevant venomous snake species. This was done to validate that a dose-dependent assay signal reduction could be obtained for cytotoxic snake venoms. The venoms of eight different snake species were selected to validate the VD assay. Each venom was tested at six different concentrations (i.e., final concentrations of 100–0.4 μg/mL) and kinetically measured for the duration of 12 h at 37 °C (Fig. 1).

All venoms except that of *D. polylepis* showed a notable egg yolk vesicle degrading effect (Fig. 2). In particular, the two highest concentrations of *B. jararaca* and the three highest concentrations of *C. rhodostoma* gave a decrease in signal similar to that of the positive control. The venom of *D. russelii* was also potent in this regard, and although the total signal reduction was less compared to *B. jararaca* and *C. rhodostoma*, the reduction could be observed for all concentrations,
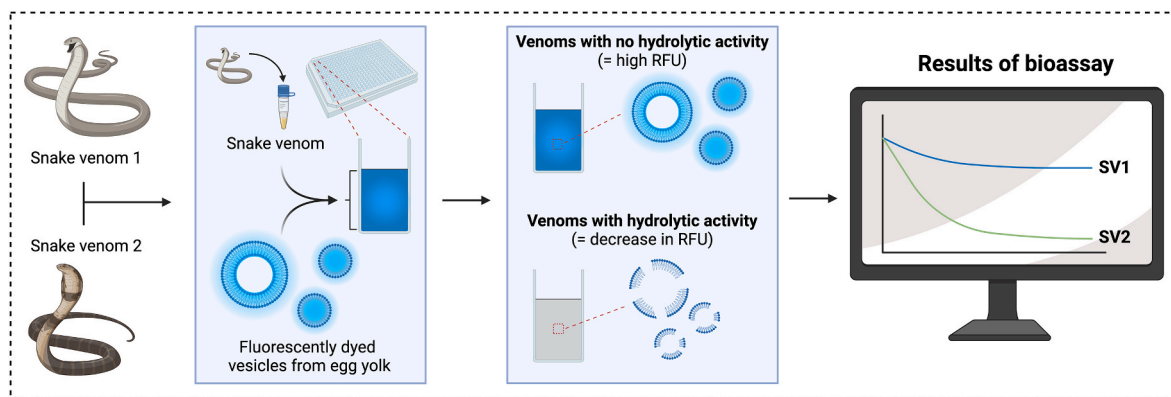
Fig. 1. The concept of using fluorescently dyed phospholipid vesicles as a proxy for membrane disruption. Graphical overview of the concept of the VD assay. RFU = relative fluorescence units. Image created using www.biorender.com.
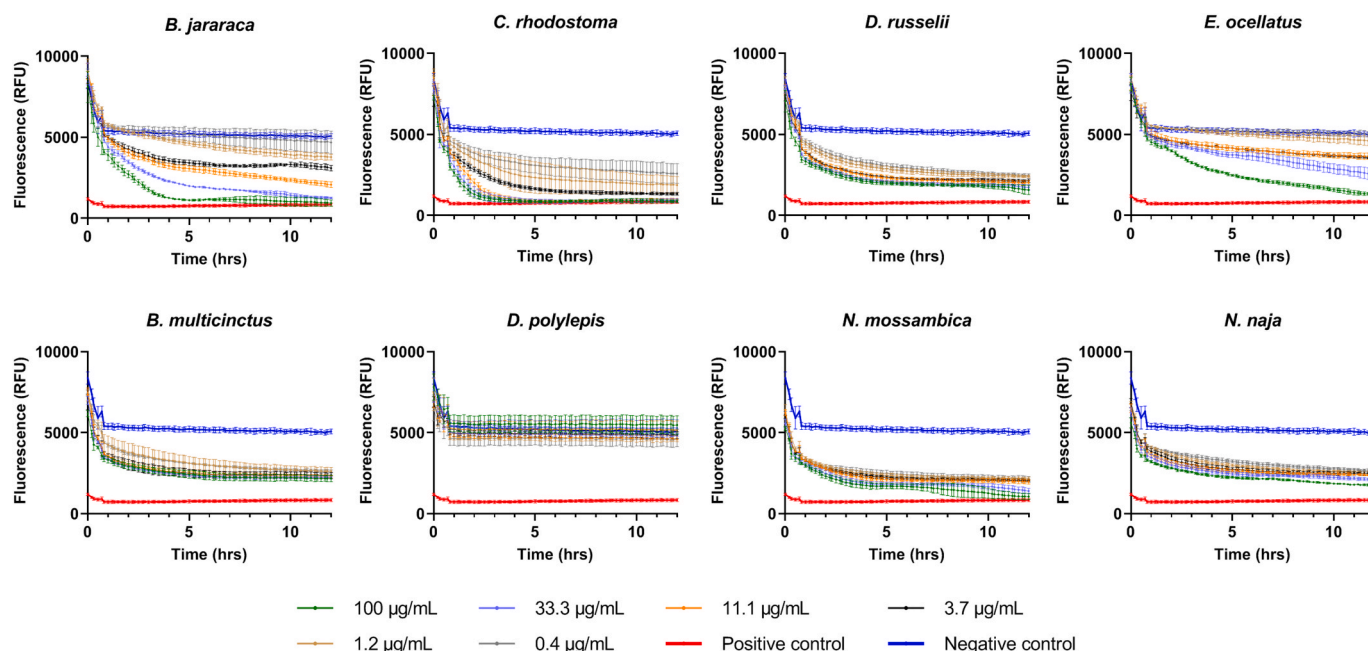

Fig. 2. Assay validation using a panel of snake venoms to study vesicle degradation. The degradation of egg yolk vesicles was monitored over 12 h (data captured every 10 min) at 37 °C, with six concentrations of venom (100–0.4 μg/mL). Ultrapure water was added as a negative control, and 2% Triton-X was added as a positive control. Readings were performed on a CLARIOstar Plus Microplate reader (using bottom optic reading); data was measured in triplicate; error bars show standard deviation.

not exclusively the highest venom concentrations. A similar effect was observed for the venoms of *B. multicinctus*, *N. mossambica* and *N. naja*. Of the elapid species that were tested, *N. mossambica* clearly had the highest effect in terms of vesicle degradation (Fig. 2).

3.4. Testing the ability of the assay to be used for neutralisation studies

In an attempt to test the versatility of the VD assay, we assessed the possible use of the assay for neutralisation studies. To do so, we tested the neutralising capacities of varespladib, as it is known for its ability to neutralise the hydrolysing effect of PLA$_2$s in snake venoms, which couVD be causing the observed egg yolk vesicles degrading effects. Varespladib acts as a potent inhibitor of venom PLA$_2$s, thereby preventing the breakdown of phospholipids in cell membranes (Gutiérrez et al., 2021; Lewin et al., 2016).

For all venoms that showed egg yolk vesicle degrading activity, we saw a significant reduction in the activity when venom was preincubated with 20 μM of varespladib (for an overview of the neutralising effects of varespladib compared to venom controls, see fig. 3 and S7 figure). Vesicle degrading activity can be observed for the highest concentrations of *B. jararaca*, *D. russelii*, *B. multicinctus* and *N. mossambica*, although to a much lesser extent. These outcomes suggest that PLA$_2$s are likely involved in egg yolk vesicle degradation observed without the inhibitor varespladib (Fig. 2). This is in line with previous studies focusing on the membrane-disrupting effect of PLA$_2$s in snake venoms. These toxins disrupt the membrane by hydrolysis of the phospholipids (in the case of enzymatically active toxins), whereas the enzymatically inactive PLA$_2$ homologs exert their effects via perturbation of the plasma membrane (Montecucco et al., 2008; Lomonte, 2023).

These findings are further supported by looking at the relative abundances of PLA$_2$s in each of the venoms. Although the venoms of *B. jararaca* and *C. rhodostoma* showed a higher potency at higher concentrations compared to *D. russelii*, the latter was consistently potent at all concentrations, with a slight increase in potency upon increasing venom concentration. When looking at the relative PLA$_2$s abundances in these venoms, we observed that *D. russelii* has the highest abundance of

PLA$_2$s (32.8–35%) compared to the other viper venoms based on literature (S2 Table). For the elapid venoms, we see that for *D. polylepis*, which contains <0.1% PLA$_2$s, no significant egg yolk vesicle degrading activity is observed (S2 Table). In contrast, for the other elapid species, which do contain much larger abundances of PLA$_2$s, we clearly see the egg yolk vesicle degrading activity that is neutralised by the PLA$_2$ inhibitor varespladib (Fig. 3).

3.5. Identification of bioactive compounds in fractioned venoms

In an effort to identify the venom components responsible for the observed vesicle degrading activity, we separated and fractionated the venoms of *C. rhodostoma* and *N. mossambica,* followed by post-column bioassaying and characterisation using HT venomics. We selected these two species as their venoms proved to be the most potent on the VD assay (Figs. 2 and 3). For parallel identification of the bioactive toxins after fractionation and bioassaying, we applied the HT venomics approach developed by Slagboom et al. (2023). The VD assay was carried out on the fractionated toxins (on the 384 V-bottom plates) after vacuum freeze-drying these overnight. The plates were measured at various time points (i.e., 0, 2, 4, 8 and 16 h), and bioassay chromatograms were generated for all time points (Fig. 4, fig. 5 and S8 figure). The baseline signal (i.e., no vesicle degrading effect) is provided on the y-axis, whereas the negative peaks (dips) correspond to bioactive fractions.
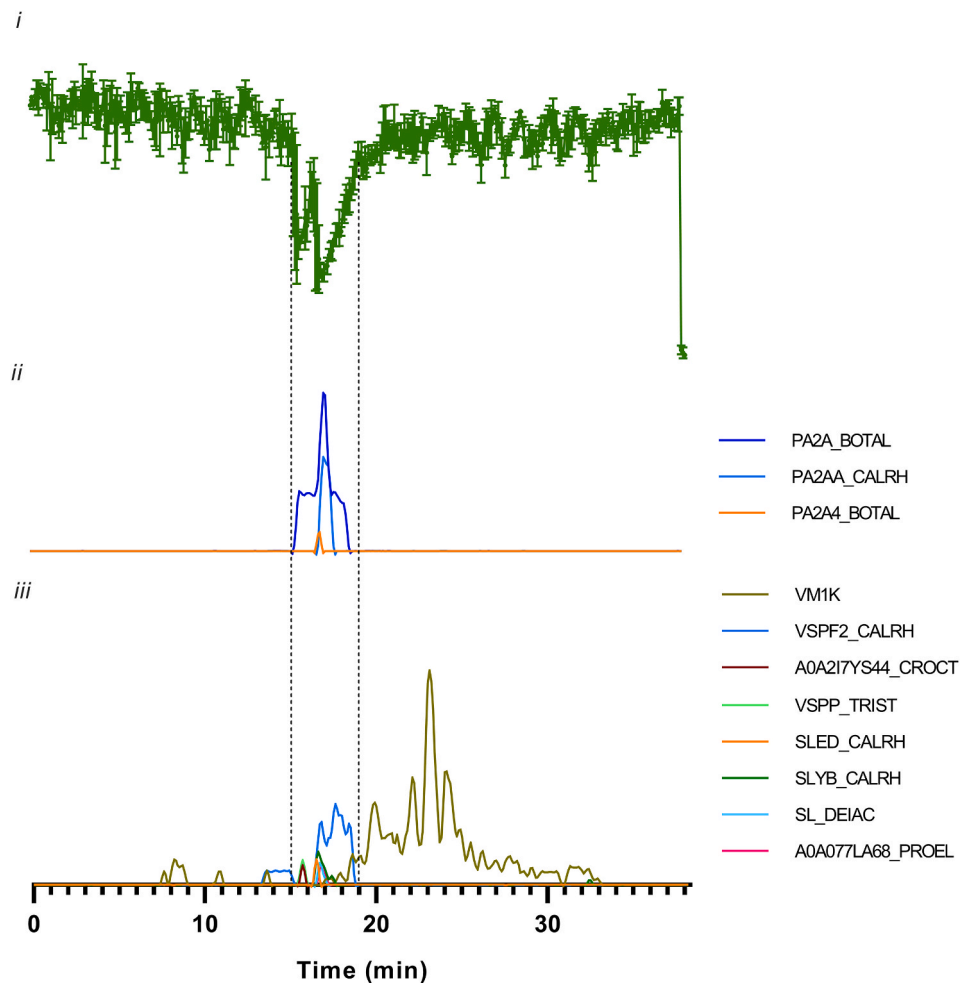
Fig. 4 shows the bioactivity chromatograms (Fig. 4i) and bioactive fractions (Fig. 4 ii and iii) for *C. rhodostoma* after 8 h of incubation. Two bioactivity peaks could be observed between 15.1 and 19.1 min. When looking at the HT venomics data (Fig. 4ii and 4iii), we identified a total of 11 toxins that matched in the retention time profile with the bioactivity peak(s) and, as such, could be identified within this bioactivity window. Of these toxins, three were found to be part of the PLA$_2$ family, and eight were part of other families (fig. 4, S3 Table). According to the Uniprot database, the following PLA$_2$s could be identified within this time frame: PA2A_BOTPC, PA2AA_CALRH, PA2A4_BOTAL. These are acidic PLA$_2$s with hydrolytic activity that are capable of degrading lipid membranes (Uniprot. P86456; Uniprot. Q9PVF1; Uniprot.Q9I8F8).

Snake venom PLA$_2$s can be divided into two groups based on their structural characteristics, with the PLA$_2$s in the viper family being classified as Group II PLA$_2$ (Arni and Ward, 1996). Within this group, two mechanisms of action can be found, with enzymatically active PLA$_2$s being capable of hydrolysing membrane phospholipids, whereas the enzymatically inactive toxins exert their effect via (in)direct perturbation of the plasma membrane (Montecucco et al., 2008; Lomonte, 2023; Kini, 2003). VM1K_CALRH is another toxin that was identified, which is part of the SVMP family of toxins. According to Uniprot, this toxin 'inhibits platelet aggregation' but is devoid of any membrane-disrupting activity (Escalante et al., 2011; Herrera et al., 2015; Uniprot. P0CB14). Other toxins that were found within the bioactivity window include several snake venom serine proteases (i.e., VSPF2_CALRH and VSPP_Trist and A0A2I7YS44_CROCT) capable of affecting haemostasis but are lacking any membrane-disrupting activity (Serrano, 2013; Uniprot. A0A2I7YS44; Uniprot.P47797; Uniprot.Q71QH7). Similarly, the snaclecs (snake C-type lectins) that were identified (SLED_CALRH; SLYB_CALRH; SL_DEIAC and A0A077LA68_PROEL) are capable of affecting normal blood coagulation, although a range of other effects (including cytotoxicity on various cancer cell lines) have been described (De Carvalho et al., 2001; Sarray et al., 2007; Uniprot. A0A077LA68; Pires et al., 2017; Sartim and Sampaio, 2015; Nunes et al., 2012; Pathan et al., 2017; Cummings and McEver, 2009; Uniprot. D2YW40; Uniprot. Q8JIV8; Uniprot. Q9I840). Most of the toxins not belonging to the family of venom PLA$_2$s are likely, not active in the egg yolk vesicle bioassay and coeluted with the tentatively identified PLA$_2$s.

Fig. 5 shows the bioactivity chromatograms (Fig. 5i) and bioactive fractions (Fig. 5 ii and iii) for *N. mossambica* after 8 h of incubation. Egg yolk vesicle degrading activity was observed between 15.1 and 19.1 min, and within this bioactivity window, a total of 12 toxins were found from HT venomics. Three toxins found were part of the PLA$_2$s family, four toxins belong to the 3FTxs family and five were found to be nerve growth factors (fig. 5, S4 Table). According to Uniprot, these PLA$_2$s are 'capable of hydrolysing phospholipids and have several activities including (in)direct haemolytic action, myonecrosis and strong anticoagulant activity' (Uniprot.P00602; Uniprot.P00603; Uniprot.P00604). In addition, the 3FTx proteins found are known, according to Uniprot,
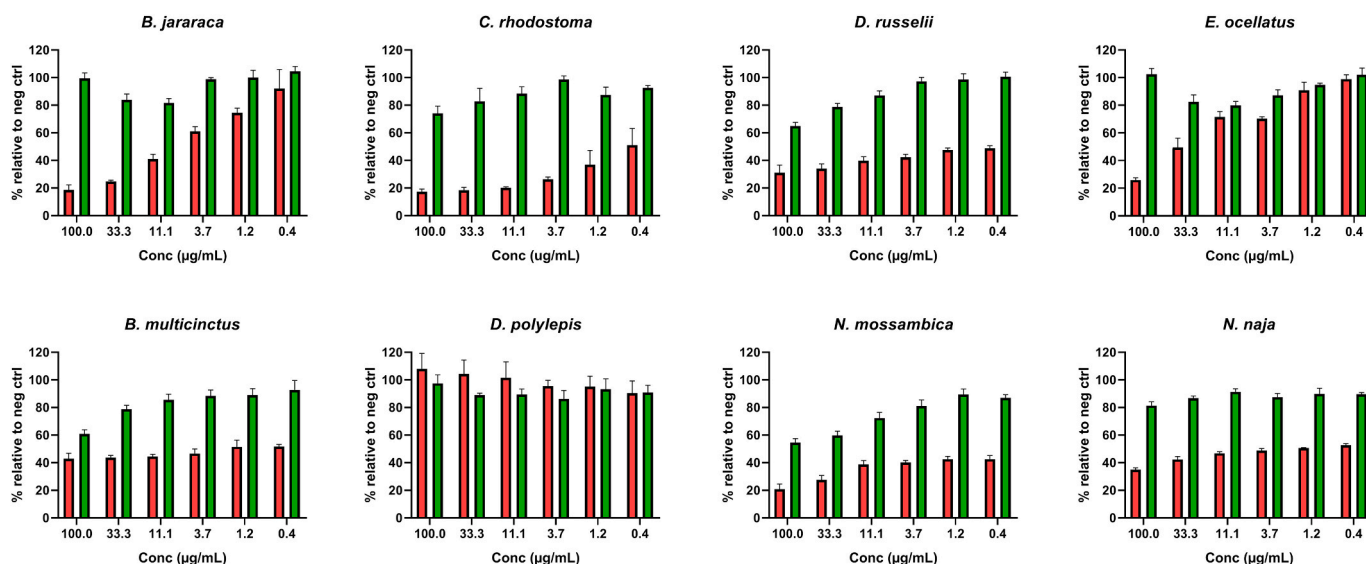
Fig. 3. Overview of the neutralising effects of varespladib on vesicle degradation evoked by different snake venoms, relative to negative control. The degradation of egg yolk vesicles after 12 h of incubation at 37 °C, with and without varespladib, is shown in the green and red bars, respectively. Results from each venom are represented in a graph, in which the vesicle degradation of six venom concentrations (100–0.4 μg/mL) is given for which the venoms are either pre-incubated with 20 μM of varespladib or, in the absence of varespladib. Negative control values were 5078 ± 145 RFU (i.e., no venom, no varespladib) and 4795 ± 43 RFU (i.e., no venom, with varespladib control). Readings were performed on a CLARIOstar microplate reader (using bottom optic reading). Data was measured in triplicate; error bars show standard deviation. (For interpretation of the references to colour in this figure legend, the reader is referred to the Web version of this article.)
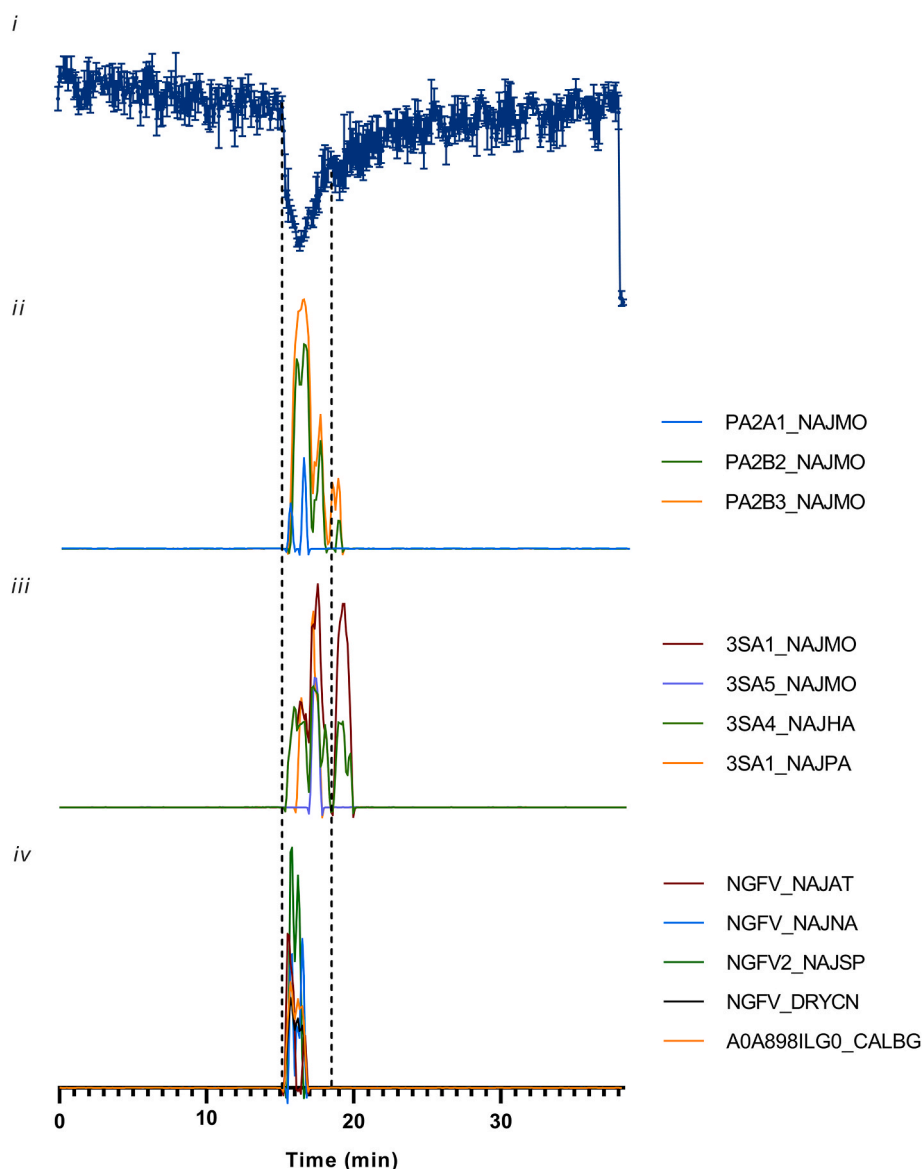
Fig. 4. Identification of bioactive fractions of C. rhodostoma venom (1 mg/mL injected) by correlating bioactivity data with high throughput venomics data. i: bioactivity chromatograms of the VD assay after 8 h of incubation of egg yolk emulsions with venom fractions at 37 °C. Peaks with negative minima indicate the presence of bioactive fractions; ii and iii: Graphs representing the protein score chromatograms (PSCs), showing the individual venom proteins found with Mascot database searching of the tryptically digested and bottom-up proteomics analysed well fractions. NB. The PSCs in ii represent PLA$_2$s correlating in retention time frame with the bioactivity peaks, and the PSCs in iii represent other protein hits. The two vertical dotted lines mark the bioactivity window, which includes the main activity peaks and their corresponding PSC peaks. The last three data points (38.1–38.3 min) show the positive control (2% Triton-X). Measurements represented by the bioactivity chromatograms were performed in triplicate; error bars show standard deviation. The corresponding CSV and Excel files can be found in the Supplementary Information folders "CSV files" and "Excel files".

for their 'cytolytic activity on different cell types by forming pores in lipid membranes'. However, the exact mechanisms by which these toxins exert their effects remain unclear (Uniprot. P01467; Uniprot. P25517; Uniprot. P01461; Uniprot. P01468). The observed effects could, therefore, also be (partially) caused by cytotoxic 3FTxs, in addition to the activity caused by PLA$_2$ toxins or by a synergistic effect between both toxin classes, which potentiates the cytotoxic effects of PLA$_2$s (Klibansky et al., 1968; Louw and Visser, 1978; Bougis et al., 1987; Chaim-matyas and Ovadia, 1987; Pucca et al., 2020; Kazandjian et al., 2021; Condrea et al., 1964). However, taking into account the vesicle degrading activity was completely neutralised by varespladib, it is also possible that PLA$_2$s are exclusively responsible for the observed effect. A third group of toxins identified within the bioactivity peak area of the venom analysed was the group of nerve growth factors. Although their exact relevance in the snake venom is not yet clear, their role in membrane disruption seems limited (Kostiza, 1996; Trummal et al., 2011; Uniprot. P61898; Uniprot. P01140) and it is likely that these toxins were non active and coeluting with the other bioactive toxins identified.

4. Concluding remarks

In this study, we describe the development of a screening assay that can be used to assess membrane degrading activities of (snake) venoms. Our goal was to develop an assay that uses a low assay volume on high-density well plates (i.e., 384 wells) and which can be used to monitor membrane degradation of crude snake venoms and fractionated venom toxins. By fluorescently dyeing the vesicles, we were able to both visualise the degradation under a fluorescence microscope and quantify the membrane degrading activity on a fluorescence plate reader. For optimisation of the VD assay, we evaluated various parameters, including the concentration of the egg yolk emulsion, well volumes, egg yolk buffer preparation methods, microwell plate types and plate reader types. Validating the assay with serial dilutions of venoms of a panel of medically relevant snake species showed that the assay could indeed be used for evaluating membrane-disrupting effects of snake venoms. The results showed a dose-dependent egg yolk vesicle degrading activity for all cytotoxic venoms investigated. The non-cytotoxic venom of *D. polylepis* did not show any activity in the bioassay. We further noticed that elapid venoms, in general, were potent across all concentrations, whereas the viper venoms showed only higher potency at the highest

Fig. 5. Identification of bioactive fractions of N. mossambica venom (1 mg/mL injected) by correlating bioactivity data with high throughput venomics data. i: bioactivity chromatograms of the VD assay after 8 h of incubation of egg yolk emulsions with venom fractions at 37 °C. Peaks with negative minima indicate the presence of bioactive fractions; ii - iii: Graphs representing the protein score chromatograms (PSCs), showing the individual venom proteins found with Mascot database searching of the tryptically digested and bottom-up proteomics analysed well fractions. NB. The PSCs in ii represent PLA$_2$s hits, iii these represent 3FTx correlating in retention time frame with the bioactivity peak, and in iv these represent other protein hits. The two dotted lines mark the bioactivity window, which includes the main activity peaks and their corresponding PSC peaks. The last three data points (38.1–38.3 min) show the positive control (2% Triton-X). Measurements represented by the bioactivity chromatograms were performed in triplicate; error bars show standard deviation. The corresponding CSV and Excel files can be found in the Supplementary Information folders "CSV files" and "Excel files".

venom concentrations tested. Further experiments which focused on the applicability of the VD assay for neutralisation studies showed that micromolar concentrations of the PLA2-inhibitor varespladib resulted in near-complete neutralisation of the observed membrane-disrupting effects for all cytotoxic venoms tested. This suggests that the observed vesicle degrading effect could be caused exclusively by PLA$_2$s. This could mean that the vesicle degradation assay would be suitable for specifically monitoring PLA2 activity.

This is further supported when we take into account the HT venomics data. When looking at the toxins identified in the venom of *C. rhodostoma*, we see that PLA$_2$s are likely to be responsible for the vesicle degrading activity, as the other toxins found are devoid of any membrane-disrupting activities. For the venom of *N. mossambica,* we expect a similar role for the PLA$_2$s, although 3FTxs might also be responsible for the vesicle degrading effect, either alone or in synergy

with PLA$_2$s. However, given the fact that the activity in crude venom is almost completely abrogated in the presence of the PLA$_2$ inhibitor varespladib, it might well be that the vesicle degrading activity is exclusively caused by PLA$_2$s. Despite these findings, it is not possible to say with complete certainty that the VD assay is specific for monitoring the vesicle degrading activities of PLA$_2$s exclusively.

The cell- and tissue-damaging effects of snake venom toxins play a major role in morbidities caused by snakebites. Therefore, it is important to develop straightforward and high-throughput assays that can be used to study these effects and for future neutralisation studies. This study was an effort to contribute new bioassaying tools for this endeavour.

Ethical statement

Not applicable.

CRediT authorship contribution statement

Mátyás A. Bittenbinder: Writing – review & editing, Writing – original draft, Visualization, Validation, Supervision, Software, Project administration, Methodology, Investigation, Funding acquisition, Formal analysis, Data curation, Conceptualization. **Eric Wachtel:** Methodology, Formal analysis, Data curation. **Daniel Da Costa Pereira:** Methodology, Formal analysis, Data curation. **Julien Slagboom:** Formal analysis, Data curation. **Nicholas R. Casewell:** Supervision. **Paul Jennings:** Supervision, Resources. **Jeroen Kool:** Writing – review & editing, Supervision, Resources, Project administration, Investigation, Data curation, Conceptualization. **Freek J. Vonk:** Writing – review & editing, Supervision, Project administration, Investigation, Conceptualization.

Declaration of competing interest

The authors declare that they have no known competing financial interests or personal relationships that could have appeared to influence the work reported in this paper.

Data availability

Data will be made available on request.

Appendix ASupplementary data

Supplementary data to this article can be found online at https://doi.org/10.1016/j.toxcx.2024.100197.

References

Abeyrathne, E.D.N.S., Nam, K.C., Huang, X., Ahn, D.U., 2022. Egg yolk lipids: separation, characterization, and utilization. Food Sci. Biotechnol. 31, 1243–1256. https://doi.org/10.1007/s10068-022-01138-4.
Alberts, B., Hopkin, K., Johnson, A.D., Morgan, D., Raff, M., Roberts, K., et al., 2018. Essential Cell Biology: Fifth International Student Edition. WW Norton & Company.
Arni, R.K., Ward, R.J., 1996. Phospholipase A2—a structural review. Toxicon 34, 827–841. https://doi.org/10.1016/0041-0101(96)00036-0.
Uniprot. P01467 · 3SA1_NAJMO · Cytotoxin 1. [cited 14 Jul 2023]. Available: https://www.uniprot.org/uniprotkb/P01467/entry.
Bénard-Valle, M., Neri-Castro, E.E., Fry, B.G., Boyer, L., Cochran, C., Alam, M., et al., 2015. Antivenom research and development. In: Fry, B.G. (Ed.), Venomous Reptiles and Their Toxins: Evolution, Pathophysiology and Biodiscovery. Oxford University Press, New York, NY, USA, pp. 61–72.
Bittenbinder, M.A., Capinha, L., Da Costa Pereira, D., Slagboom, J., van de Velde, B., Casewell, N.R., et al., 2023. Development of a high-throughput in vitro screening method for the assessment of cell-damaging activities of snake venoms. PLoS Negl Trop Dis 17, e0011564. https://doi.org/10.1371/journal.pntd.0011564.
Bougis, P.E., Marchot, P., Rochat, H., 1987. In vivo synergy of cardiotoxin and phospholipase A2 from the elapid snake Naja mossambica mossambica. Toxicon 25, 427–431. https://doi.org/10.1016/0041-0101(87)90076-6.
Bryan-Quirós, W., Fernández, J., Gutiérrez, J.M., Lewin, M.R., Lomonte, B., 2019. Neutralizing properties of LY315920 toward snake venom group I and II myotoxic phospholipases A2. Toxicon 157, 1–7. https://doi.org/10.1016/j.toxicon.2018.11.292.
Bucevičius, J., Lukinavičius, G., Gerasimaite, R., 2018. The Use of Hoechst dyes for DNA staining and beyond. Chemosens 6, 18. https://doi.org/10.3390/CHEMOSENSORS6020018, 2018;6: 18.
Uniprot. P25517 · 3SA5_NAJMO · Cytotoxin 5. [cited 14 Jul 2023]. Available: https://www.uniprot.org/uniprotkb/P25517/entry.
Chaim-matyas, A., Ovadia, M., 1987. Cytotoxic activity of various snake venoms on melanoma, B16F10 and Chondrosarcoma. Life Sci. 40, 1601–1607.
Chippaux, J.P., 2017. Snakebite envenomation turns again into a neglected tropical disease. J. Venom. Anim. Toxins Incl. Trop. Dis. 23, 1–2. https://doi.org/10.1186/s40409-017-0127-6.
Condrea, E., De Vries, A., Mager, J., 1962. Action OF snake-venom phospholipase a ON free and LIPOPROTEIN-BOUND phospholipids. Biochim. Biophys. Acta 58, 389–397.

Condrea, E., De Vries, A., Mager, J., 1964. Hemolysis and splitting of human erythrocyte phospholipids by snake venoms. BBA - Spec Sect Lipids Relat Subj 84, 60–73. https://doi.org/10.1016/0926-6542(64)90101-5.
Cummings, R.D., McEver, R.P., C-type Lectins, 2009. In: Essentials of Glycobiology Cold Spring Harbor Laboratory Press. Cold Spring Harbor (NY): Cold Spring Harbor Laboratory Press. Available: https://www.ncbi.nlm.nih.gov/books/NBK1943/.
Uniprot. P01461 · 3SA4_NAJHA · Cytotoxin 4. [cited 24 Jan 2024]. Available: https://www.uniprot.org/uniprotkb/P01461/entry.
De Carvalho, D.D., Schmitmeier, S., Novello, J.C., Markland, F.S., 2001. Effect of BJcuL (a lectin from the venom of the snake Bothrops jararacussu) on adhesion and growth of tumor and endothelial cells. Toxicon 39, 1471–1476. https://doi.org/10.1016/S0041-0101(01)00106-4.
Dennis, E.A., Cao, J., Hsu, Y.H., Magrioti, V., Kokotos, G., 2011. Phospholipase A2 enzymes: physical structure, biological function, disease implication, chemical inhibition, and therapeutic intervention. Chem Rev 111, 6130–6185. https://doi.org/10.1021/cr200085w.
Doley, R., King, G.F., Mukherjee, A.K., 2004. Differential hydrolysis of erythrocyte and mitochondrial membrane phospholipids by two phospholipase A2 isoenzymes (NK-PLA2-I and NK-PLA2-II) from the venom of the Indian monocled cobra Naja kaouthia. Arch. Biochem. Biophys. 425, 1–13. https://doi.org/10.1016/j.abb.2004.02.007.
Uniprot. P01468 · 3SA1_NAJPA · Cytotoxin 1. [cited 24 Jan 2024]. Available: https://www.uniprot.org/uniprotkb/P01468/entry.
Uniprot. P61898 · NGFV_NAJAT · Venom nerve growth factor.
Escalante, T., Rucavado, A., Fox, J.W., Gutiérrez, J.M., 2011. Key events in microvascular damage induced by snake venom hemorrhagic metalloproteinases. J Proteomics 74, 1781–1794. https://doi.org/10.1016/j.jprot.2011.03.026.
Uniprot. P01140. NGFV_NAJNA · Venom nerve growth factor [cited 24 Jan 2024]. Available: https://www.uniprot.org/uniprotkb/P01140/entry.
Fernandes, F.F.A., Tomaz, M.A., El-Kik, C.Z., Monteiro-Machado, M., Strauch, M.A., Cons, B.L., et al., 2014. Counteraction of Bothrops snake venoms by Combretum leprosum root extract and arjunolic acid. J. Ethnopharmacol. 155, 552–562. https://doi.org/10.1016/j.jep.2014.05.056.
Fry, B.G., 2015. Venomous Reptiles and Their Toxins: Evolution, Pathophysiology and Biodiscovery. Oxford University Press, Oxford University Press. https://doi.org/10.1016/0041-0101(71)90017-1.
Gasanov, S.E., Dagda, R.K., Rael, E.D., 2014. Snake venom cytotoxins, phospholipase A2 s, and Zn2+ -dependent metalloproteinases: mechanisms of action and Pharmacological relevance. J. Clin. Toxicol. 4.
Gopalakrishnakone, P., Inagaki, H., Vogel, C., Mukherjee, A.K., Rahmy, T.R., 2017. Snake Venoms. Springer, Berlin, Germany.
Gutiérrez, J.M., Escalante, T., Rucavado, A., Herrera, C., Fox, J.W., 2016. A comprehensive view of the structural and functional alterations of extracellular matrix by snake venom metalloproteinases (SVMPs): Novel perspectives on the pathophysiology of envenoming. Toxins 8. https://doi.org/10.3390/toxins8100304.
Gutiérrez, J.M., Calvete, J.J., Habib, A.G., Harrison, R.A., Williams, D.J., Warrell, D.A., 2017. Snakebite envenoming. Nat. Rev. Dis. Prim. 3 https://doi.org/10.1038/NRDP.2017.63.
Gutiérrez, J.M., Albulescu, L.O., Clare, R.H., Casewell, N.R., Abd El-Aziz, T.M., Escalante, T., et al., 2021. The search for natural and synthetic inhibitors that would complement antivenoms as therapeutics for snakebite envenoming. Toxins 13, 1–30. https://doi.org/10.3390/toxins13070451.
Habib, A.G., Kuznik, A., Hamza, M., Abdullahi, M.I., Chedi, B.A., Chippaux, J.P., et al., 2015. Snakebite is under appreciated: appraisal of burden from west Africa. PLoS Negl Trop Dis 9, 4–11. https://doi.org/10.1371/journal.pntd.0004088.
Herrera, C., Escalante, T., Voisin, M.B., Rucavado, A., Morazán, D., Macêdo, J.K.A., et al., 2015. Tissue localization and extracellular matrix degradation by PI, PII and PIII snake venom metalloproteinases: clues on the mechanisms of venom-induced hemorrhage. PLoS Negl Trop Dis 9, 1–20. https://doi.org/10.1371/journal.pntd.0003731.
Joubert, F.J., Taljaard, N., 1980. Purification, some properties and amino-acid sequences of two phospholipases A (CM-II and CM-III) from Naja naja kaouthia venom. Eur. J. Biochem. 112, 493–499. https://doi.org/10.1111/j.1432-1033.1980.tb06112.x.
Kasturiratne, A., Wickremasinghe, A.R., De Silva, N., Gunawardena, N.K., Pathmeswaran, A., Premaratna, R., et al., 2008. The global burden of snakebite: a literature analysis and modelling based on regional estimates of envenoming and deaths. PLoS Med. 5, 1591–1604. https://doi.org/10.1371/journal.pmed.0050218.
Kazandjian, T.D., Petras, D., Robinson, S.D., van Thiel, J., Greene, H.W., Arbuckle, K., et al., 2021. Convergent evolution of pain-inducing defensive venom components in spitting cobras. Science (80-) 371, 386–390. https://doi.org/10.1126/science.abb9303.
Kini, R.M., 2003. Excitement ahead: structure, function and mechanism of snake venom phospholipase A2 enzymes. Toxicon 42, 827–840. https://doi.org/10.1016/j.toxicon.2003.11.002.
Klibansky, C., London, Y., Frenkel, A., De Vries, A., 1968. Enhancing action of synthetic and natural basic polypeptides on erythrocyte-ghost phospholipid hydrolysis by phospholipase A. Biochim Biophys Acta - Biomembr 150, 15–23. https://doi.org/10.1016/0005-2736(68)90003-5.
Kostiza, T., 1996. Neurotrophic factors are endogenous soluble proteins regulating survival , growth , morphological plasticity , or synthesis of proteins for differentiated functions of neurons. The. Science (80-) 34, 787–806.
Lalande, M.E., Ling, V., Miller, R.G., 1981. Hoechst 33342 dye uptake as a probe of membrane permeability changes in mammalian cells. Proc Natl Acad Sci U S A 78, 363–367. https://doi.org/10.1073/pnas.78.1.363.
Lewin, M., Samuel, S., Merkel, J., Bickler, P., 2016. Varespladib (LY315920) appears to be a potent, broad-spectrum, inhibitor of snake venom phospholipase A2 and a

possible pre-referral treatment for envenomation. Toxins 8. https://doi.org/10.3390/toxins8090248.

Lewin, M.R., Carter, R.W., Matteo, I.A., Samuel, S.P., Rao, S., Fry, B.G., et al., 2022. Varespladib in the treatment of snakebite envenoming: development history and preclinical evidence supporting advancement to clinical trials in patients bitten by venomous snakes. Toxins 14, 1–21. https://doi.org/10.3390/toxins14110783.

Lomonte, B., 2023. Lys49 myotoxins, secreted phospholipase A2-like proteins of viperid venoms: a comprehensive review. Toxicon 224, 107024. https://doi.org/10.1016/j.toxicon.2023.107024.

Longbottom, J., Shearer, F.M., Devine, M., Alcoba, G., Chappuis, F., Weiss, D.J., et al., 2018. Vulnerability to snakebite envenoming : a global mapping of hotspots. Lancet 392, 673–684. https://doi.org/10.1016/S0140-6736(18)31224-8.

Louw, A.I., Visser, L., 1978. The synergism of cardiotoxin and phospholipase A2 in hemolysis. BBA - Biomembr. 512, 163–171. https://doi.org/10.1016/0005-2736(78)90227-4.

Marinetti, G.V., 1965. The action of phospholipase A on lipoproteins. Biochim Biophys Acta (BBA)/Lipids Lipid Metab 98, 554–565. https://doi.org/10.1016/0005-2760(65)90152-9.

Markland, F.S., Swenson, S., 2013. Snake venom metalloproteinases. Toxicon 62, 3–18. https://doi.org/10.1016/j.toxicon.2012.09.004.

Mladic, M., Zietek, B.M., Iyer, J.K., Hermarij, P., Niessen, W.M.A., Somsen, G.W., et al., 2016. At-line nanofractionation with parallel mass spectrometry and bioactivity assessment for the rapid screening of thrombin and factor Xa inhibitors in snake venoms. Toxicon 110, 79–89. https://doi.org/10.1016/j.toxicon.2015.12.008.

Mladic, M., de Waal, T., Burggraaff, L., Slagboom, J., Somsen, G.W., Niessen, W.M.A., et al., 2017. Rapid screening and identification of ACE inhibitors in snake venoms using at-line nanofractionation LC-MS. Anal. Bioanal. Chem. 409, 5987–5997. https://doi.org/10.1007/s00216-017-0531-3.

Montecucco, C., Gutiérrez, J.M., Lomonte, B., 2008. Cellular pathology induced by snake venom phospholipase A2 myotoxins and neurotoxins: common aspects of their mechanisms of action. Cell. Mol. Life Sci. 65, 2897–2912. https://doi.org/10.1007/s00018-008-8113-3.

Monteiro, N., Martins, A., Reis, R.L., Neves, N.M., 2014. Liposomes in tissue engineering and regenerative medicine. J R Soc Interface 11. https://doi.org/10.1098/rsif.2014.0459.

Nsairat, H., Khater, D., Sayed, U., Odeh, F., Al Bawab, A., Alshaer, W., 2022. Liposomes: structure, composition, types, and clinical applications. Helliyon. Elsevier. https://doi.org/10.1016/j.heliyon.2022.e09394.

Nunes, E.S., Souza, M.A.A., Vaz, A.F.M., Silva, T.G., Aguiar, J.S., Batista, A.M., et al., 2012. Cytotoxic effect and apoptosis induction by Bothrops leucurus venom lectin on tumor cell lines. Toxicon 59, 667–671. https://doi.org/10.1016/J.TOXICON.2012.03.002.

Oladimeji, B.M., Gebhardt, R., 2023. Physical characteristics of egg yolk granules and effect on their functionality. Foods 12. https://doi.org/10.3390/foods12132531.

Palermo, G., Schouten, W.M., Alonso, L.L., Ulens, C., Kool, J., Slagboom, J., 2023. Acetylcholine-Binding protein affinity profiling of neurotoxins in snake venoms with parallel toxin identification. Int. J. Mol. Sci. 24, 16769 https://doi.org/10.3390/ijms242316769.

Pathan, J., Mondal, S., Sarkar, A., Chakrabarty, D., 2017. Daboialectin, a C-type lectin from Russell's viper venom induces cytoskeletal damage and apoptosis in human lung cancer cells in vitro. Toxicon 127, 11–21. https://doi.org/10.1016/J.TOXICON.2016.12.013.

Pires, W.L., de Castro, O.B., Kayano, A.M., da Silva Setúbal, S., Pontes, A.S., Nery, N.M., et al., 2017. Effect of BjcuL, a lectin isolated from Bothrops jararacussu, on human peripheral blood mononuclear cells. Toxicol Vitr 41, 30–41. https://doi.org/10.1016/J.TIV.2017.02.003.

Price, J.A., 2007. A colorimetric assay for measuring phospholipase A2 degradation of phosphatidylcholine at physiological pH. J. Biochem. Biophys. Methods 70, 441–444. https://doi.org/10.1016/j.jbbm.2006.10.008.

Pucca, M.B., Ahmadi, S., Cerni, F.A., Ledsgaard, L., Sørensen, C.V., McGeoghan, F.T.S., et al., 2020. Unity makes strength: exploring intraspecies and interspecies toxin synergism between phospholipases A2 and cytotoxins. Front. Pharmacol. 11, 1–10. https://doi.org/10.3389/fphar.2020.00611.

Salvador, G.H.M., Gomes, A.A.S., Bryan-Quirós, W., Fernández, J., Lewin, M.R., Gutiérrez, J.M., et al., 2019. Structural basis for phospholipase A2-like toxin inhibition by the synthetic compound Varespladib (LY315920). Sci. Rep. 9, 1–13. https://doi.org/10.1038/s41598-019-53755-5.

Sarray, S., Delamarre, E., Marvaldi, J., El, Ayeb M., Marrakchi, N., Luis, J., 2007. Lebectin and lebecetin, two C-type lectins from snake venom, inhibit α5β1 and αv-containing integrins. Matrix Biol. 26, 306–313. https://doi.org/10.1016/J.MATBIO.2007.01.001.

Sartim, M.A., Sampaio, S.V., 2015. Snake venom galactoside-binding lectins: a structural and functional overview. J. Venom. Anim. Toxins Incl. Trop. Dis. 21, 1–11. https://doi.org/10.1186/S40409-015-0038-3/TABLES/2.

Secretariat, C.B.D., 2011. Nagoya protocol on access to genetic Resources and the fair and equitable sharing of benefits arising from their utilization to the convention on biological diversity - text and annex. Nagoya Protoc 12, 1–320. Available: http://www.cites.org/common/com/PC/15/X-PC15-10-Inf.pdf.

Senji Laxme, R.R., Khochare, S., de Souza, H.F., Ahuja, B., Suranse, V., Martin, G., et al., 2019. Beyond the 'Big four': venom profiling of the medically important yet neglected Indian snakes reveals disturbing antivenom deficiencies. PLoS Negl Trop Dis 13, e0007899. https://doi.org/10.1371/journal.pntd.0007899.

Senji Laxme, R.R., Attarde, S., Khochare, S., Suranse, V., Martin, G., Casewell, N.R., et al., 2021. Biogeographical venom variation in the indian spectacled cobra (Naja naja) underscores the pressing need for pan-India efficacious snakebite therapy. PLoS Negl Trop Dis 15, 1–28. https://doi.org/10.1371/journal.pntd.0009150.

Serrano, S.M.T., 2013. The long road of research on snake venom serine proteinases. Toxicon 62, 19–26. https://doi.org/10.1016/j.toxicon.2012.09.003.

Slagboom, J., Kool, J., Harrison, R.A., Casewell, N.R., 2017. Haemotoxic snake venoms: their functional activity, impact on snakebite victims and pharmacological promise. Br. J. Haematol. 177, 947–959. https://doi.org/10.1111/bjh.14591.

Slagboom, J., Derks, R.J.E., Sadighi, R., Somsen, G.W., Ulens, C., Casewell, N.R., et al., 2023. High-throughput venomics. J. Proteome Res. 22, 1734–1746. https://doi.org/10.1021/acs.jproteome.2c00780.

Still, K.B.M., Slagboom, J., Kidwai, S., Xie, C., Zhao, Y., Eisses, B., et al., 2020. Development of high-throughput screening assays for profiling snake venom phospholipase A2 activity after chromatographic fractionation. Toxicon 184, 28–38. https://doi.org/10.1016/j.toxicon.2020.05.022.

Strixner, T., Sterr, J., Kulozik, U., Gebhardt, R., 2014. Structural study on hen-egg yolk high density lipoprotein (HDL) granules. Food Biophys. 9, 314–321. https://doi.org/10.1007/s11483-014-9359-y.

Sunagar, K., Jackson, T.N.W., Undheim, E.A.B., Ali, S.A., Antunes, A., Fry, B.G., 2013. Three-fingered RAVERs: rapid accumulation of variations in exposed residues of snake venom toxins. Toxins 5, 2172–2208. https://doi.org/10.3390/toxins5112172.

Trummal, K., Tõnismägi, K., Paalme, V., Järvekülg, L., Siigur, J., Siigur, E., 2011. Molecular diversity of snake venom nerve growth factors. Toxicon 58, 363–368. https://doi.org/10.1016/j.toxicon.2011.07.005.

Uniprot. P86456 · PA2A4_BOTAL · Acidic phospholipase A2 SpII RP4. Available: https://www.uniprot.org/uniprotkb/P86456/entry.

Uniprot. Q9PVF1 · PA2AA_CALRH · Acidic phospholipase A2 S1E6-a. [cited 24 Jan 2024]. Available: https://www.uniprot.org/uniprotkb/Q9PVF1/entry.

Uniprot. A0A2I7YS44. A0A2I7YS44_CROCT · Serine endopeptidase [cited 24 Jan 2024]. Available: https://www.uniprot.org/uniprotkb/A0A2I7YS44/entry.

Uniprot.Q9I8F8 · PA2A_BOTPC · Acidic phospholipase A2. [cited 24 Jan 2024]. Available: https://www.uniprot.org/uniprotkb/Q9I8F8/entry.

Uniprot. A0A077LA68 · A0A077LA68_PROEL · Galactose-binding Lectin. [cited 24 Jan 2024]. Available: https://www.uniprot.org/uniprotkb/A0A077LA68/entry.

Uniprot. D2YW40 · SLED_CARLH · Snaclec rhodocetin subunit delta. [cited 24 Jan 2024]. Available: https://www.uniprot.org/uniprotkb/D2YW40/entry.

Uniprot. P0CB14 · VM1K_CALRH · Snake venom metalloproteinase kistomin. [cited 24 Jan 2024]. Available: https://www.uniprot.org/uniprotkb/P0CB14/entry.

Uniprot. Q8JIV8 · SL_DEIAC · Snaclec clone 2100755. [cited 24 Jan 2024]. Available: https://www.uniprot.org/uniprotkb/Q8JIV8/entry.

Uniprot. Q9I840 · SLYB_CALRH · Snaclec rhodocetin subunit beta. [cited 24 Jan 2024]. Available: https://www.uniprot.org/uniprotkb/Q9I840/entry.

Uniprot.P00602 · PA2A1_NAJMO · Acidic phospholipase A2 CM-I. [cited 14 Jul 2023]. Available: https://www.uniprot.org/uniprotkb/P00602/entry.

Uniprot.P00603 · PA2B2_NAJMO · Basic phospholipase A2 CM-II. [cited 14 Jul 2023]. Available: https://www.uniprot.org/uniprotkb/P00603/entry.

Uniprot.P00604 · PA2B3_NAJMO · Basic phospholipase A2 CM-III. [cited 14 Jul 2023]. Available: https://www.uniprot.org/uniprotkb/P00604/entry.

Uniprot.P47797 · VSPF2_CALRH · Thrombin-like enzyme ancrod-2. [cited 24 Jan 2024]. Available: https://www.uniprot.org/uniprotkb/P47797/entry.

Warrell, D.A., 2010. Guidelines of management of snake bite. Lancet 375, 77–88. https://doi.org/10.1016/S0140-6736(09)61754-2.

Zietek, B.M., Mayar, M., Slagboom, J., Bruyneel, B., Vonk, F.J., Somsen, G.W., et al., 2018. Liquid chromatographic nanofractionation with parallel mass spectrometric detection for the screening of plasmin inhibitors and (metallo)proteinases in snake venoms. Anal. Bioanal. Chem. 410, 5751–5763. https://doi.org/10.1007/s00216-018-1253-x.

Uniprot.Q71QH7 · VSPP_TRIST · Snake venom serine protease PA. [cited 24 Jan 2024]. Available: https://www.uniprot.org/uniprotkb/Q71QH7/entry.